Properties of the Dark and Signaling States of Photoactive Yellow Protein Probed by Solution Phase Hydrogen/Deuterium Exchange and Mass Spectrometry†

Guilong Cheng,‡ Michael A. Cusanovich,*,§ and Vicki H. Wysocki‡,§

Department of Chemistry and Department of Biochemistry and Molecular Biophysics, University of Arizona, Tucson, Arizona 85721

Received May 2, 2006; Revised Manuscript Received July 31, 2006

ABSTRACT: The perturbations on conversion from the dark state to the signaling state in photoactive yellow protein have been determined by solution-phase hydrogen/deuterium exchange and mass spectrometry. Both the wild type and M100A mutant are used in this study, with the mutant providing over 90% conversion to the bleached state under steady-state illumination. We found perturbations in both the wild type and the mutant on illumination, consistent with a more flexible structure in the long-lived signaling (I_2') state. In the case of the wild type, the conformational changes detected are mainly around the chromophore region. With the M100A mutant, differences in H/D exchange between the light and dark are more extensive as compared to wild type; not only are the chromophore surroundings affected, but significant increases in deuterium uptake in the N-terminus and central β-sheet are observed as well. On the basis of the data obtained from this study and previous findings, a sequence of events that leads to the perturbation of PYP following chromophore photoisomerization is proposed.

Photoactive yellow protein (PYP)[1] (*1*) is a small 14 kDa soluble cytoplasmic protein originally isolated from the halophilic purple phototrophic bacterium, *Halorhodospira (Ectothiorhodospira) halophila.* When exposed to light, the *p*-hydroxycinnamic acid chromophore undergoes a trans to cis isomerization, which initiates a set of conformational changes, leading to a signaling state (I_2') (*2*, *3*). The fast decay of the signaling state (half-life of ∼140 ms) completes the photocycle and returns PYP to its dark state. The structure of PYP in the dark state has been determined by X-ray crystallography (*4*, *5*) and NMR (*6*). In both structures, the protein is composed of a central, twisted, six-stranded antiparallel β-sheet, flanked by loops and helices on both sides. The basic structural motif is termed the PAS fold, which is found in many sensory proteins from bacteria to human (*7*, *8*). Although considerable effort has been invested to probe the changes in conformation leading to the signaling state and the pathway through which these changes occur (*5*, *9*−*13*), and different models have been proposed (*7*, *12*−*14*), no consensus has been reached. This is due, in large part, to the short lifetime of wild-type PYP in the signaling state and is further complicated by the number of intermediates existing prior to the I_2' state. Among the number of intermediate states existing before the I_2' state, only one other state, I_2, has the chromophore bleached, that is, absorbing at less than 360 nm. Thus, both I_2 and I_2' have a protonated cis chromophore, with the formation of I_2' coupled to a large structural change generating the presumed signaling state (*2*). Moreover, it has been recently shown that I_2 and I_2' are in a salt- and pH-dependent equilibrium (*15*, *16*). Intermediates prior to I_2 appear to only involve movement of the chromophore and adjacent amino acid side chains and do not result in significant structural changes (*17*). Moreover, crystallized protein does not undergo the same photocycle as in solution (*18*), a consequence of the large conformational changes required to reach the signaling state being constrained by the crystal packing forces. To gain insight into the effect of photoisomerization on the destabilization of PYP that is a consequence of the conversion to the signaling state, we have used the PYP M100A mutant, which has a long signaling state lifetime (*19*) and probed its structure with solution-phase hydrogen/deuterium exchange coupled with mass spectrometry.

MATERIALS AND METHODS

PYP Wild Type and M100A Mutant Preparation. H. halophila wild-type PYP and the M100A mutant were prepared as previously described (*20*, *21*). Both proteins were concentrated (840 μM) and stored in 10 mM sodium phosphate and 80 mM KCl (pH 6.8).

Spectroscopy. Absorption spectra were obtained with a CARY 300 spectrophotometer. To spectrally monitor the signaling state, PYP (wild type or the M100A mutant) was illuminated with a tungsten lamp (60 W) using a 410 nm cutoff filter (Corning 4-72 stacked with K-2), and the cuvette was immediately transferred to the spectrophotometer. The

† This work was supported by NIH Grant GM21277 to M.A.C., NIH Grant GM051387 to V.H.W., and the 2005−2006 Pfizer Graduate Research Fellowship in Analytical Chemistry to G.C.

* To whom correspondence should be addressed. Tel: (520) 621-7533. Fax: (520) 621-6603. E-mail: cusanovi@u.arizona.edu.

‡ Department of Chemistry, University of Arizona.

§ Department of Biochemistry and Molecular Biophysics, University of Arizona.

[1] Abbreviations: PYP, photoactive yellow protein; PAS, acronym formed from the names of the first three proteins recognized as sharing this sensor motif (*p*eriodic clock protein of *Drosophila*, *a*ryl hydrocarbon receptor nuclear translocator of vertebrates, *s*ingle-minded protein of *Drosophila*); H/D exchange, hydrogen/deuterium exchange; MS, mass spectrometry.

10.1021/bi0608663 CCC: $33.50
Published on Web 09/09/2006

absorption measurement was determined from 420 to 460 nm to minimize the impact of dark recovery. For the exchange experiments in the dark, the protein stock was incubated in the dark for 30 min prior to exchange and incubated in a dark room with a dim red light for the duration of exchange. In the light experiments, PYP solutions were illuminated with blue light for the duration of the sampling period described in the next section. The cuvette was thermostated in a copper cuvette holder with circulating water to eliminate temperature drift due to illumination for long periods of time.

Peptide Mapping of PYP Wild Type and the M100A Mutant by HPLC−Tandem Mass Spectrometry. A total of 200 pmol of protein stock was diluted into 10 mM sodium phosphate and 80 mM KCl (pH 6.8) to a final concentration of 20 μM, followed by 1:1 mixing with 100 mM sodium phosphate and 4 M guanidinium chloride (pH 2.2). The sample was applied to a column of immobilized pepsin [2 mm × 50 mm, packed in house (*22*)] using water and 0.05% TFA as the mobile phase. The protein digest was collected by a micropeptide trap (Michrome BioResources, Auburn, CA) and washed for 2 min. Peptides in the trap were then eluted from the trap onto a microbore C-18 HPLC column (1 mm × 50 mm; Micro-Tech Scientific, Vista, CA) coupled to a Waters micro Q-TOF (Milford, MA) for accurate parent mass measurements. Peptides were eluted from the column in 7 min using a gradient of 15−45% acetonitrile at a flow rate of 50 μL/min. The micropeptide trap and HPLC column were immersed in ice water during the entire process. The same experiment was repeated using a Finnigan LCQ Classic quadrupole ion trap mass spectrometer (Thermo Electron Corp., Waltham, MA) in data-dependent mode to acquire product (tandem) MS spectra. Both parent mass and tandem mass spectra were used for peptide identification. The Waters micro Q-TOF was subsequently used for all H/D exchange measurements.

Hydrogen/Deuterium Exchange. Hydrogen exchange experiments were initiated by diluting the concentrated protein stock (∼42-fold) into the labeling solution (D_2O, 5 mM sodium phosphate, pD 6.8) to a final concentration of 20 μM. Incubation times ranged from 30 s to 8 h. All pH and pD values reported were taken directly from the pH meter and were not corrected for isotope effects (*23*). At each time point, an aliquot of 250 pmol of protein was taken out of the exchange tube and quenched by mixing the solution in a 1:1 ratio with the quenching buffer [D_2O, 100 mM sodium phosphate, 4 M guanidine deuterium chloride (pD 2.2)].

Hydrogen Exchange Analysis by HPLC-ESI. The samples for peptide analysis were treated as described for the unlabeled protein in the peptide mapping section. The intact protein samples were analyzed similarly to the protein digest, with three exceptions. The pepsin column was not used for the MS experiment with intact protein, the micropeptide trap was replaced by a microprotein trap (Michrom BioResources, Auburn, CA), and 60% acetonitrile was used for protein elution. Mass spectrometry analyses of all samples within each comparison set were done on the same day with the same instrumental conditions. Deconvolution of intact protein spectra was performed with the program MaxEnt1 (Waters). The error of each data point for the intact protein was determined to be ±3 Da based on multiple measurements. The mass of each peptide was taken as the centroid mass of the isotopic envelope with the program MagTran (*24*). The error of each data point for the peptides was determined to be ±0.3 Da based on multiple measurements.

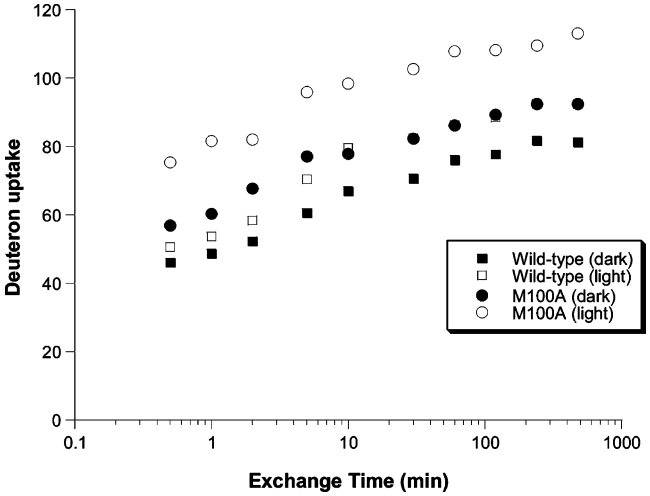

FIGURE 1: Deuterium uptake by intact wild-type and M100A PYP as a function of time. Filled squares and circles: wild-type and M100A PYP exchanged in the dark, respectively. Open squares and circles: wild-type and M100A PYP exchanged with steady-state blue light illumination, respectively. Filled circles and open squares overlap after 30 min. Exchange conditions: 5 mM sodium phosphate, pD 6.8.

In order to account for the exchange of deuterium during the HPLC step (back-exchange) and the use of only 42-fold excess deuterium oxide during the labeling step, which limits the forward exchange reaction, an experimental correction is necessary. In our experiments, a 100% deuterated protein control was prepared by diluting the protein stock in the labeling solution and quenching buffer, incubating at 60 °C for 3 h, and then incubating at room temperature (approximately 22 °C) for >24 h. The corrected extent of deuterium incorporation was calculated according to the equation (*25*, *26*):

$$m = \frac{m_{\mathrm{exp}} - m_{0\%}}{m_{100\%} - m_{0\%}} N \qquad (1)$$

where m_{exp} is the experimental centroid mass of the peptide at a certain time point, $m_{0\%}$ is the centroid mass of the undeuterated control, $m_{100\%}$ is the centroid mass of the 100% deuterated control, and N is the number of amide hydrogens for each peptide characterized.

RESULTS

Intact Protein Exchange Kinetics. Deuterium uptake by intact wild type and M100A in the dark and with blue light illumination is shown in Figure 1. As can be seen, both the wild type and M100A exchange more amide hydrogens under blue light illumination than in the dark. Moreover, in the dark, the M100A mutant exchanges more amide hydrogens relative to the wild-type protein. Note, however, that the steady-state level of the signaling state is quite different for wild type as compared to M100A. With wild-type PYP, less than 10% of the protein is estimated to be in the I_2 states (I_2 and I_2') based on the loss of 445 nm absorbance on steady-state illumination with blue light, a consequence of the rapid recovery of the signaling state (lifetime of ∼140 ms) back

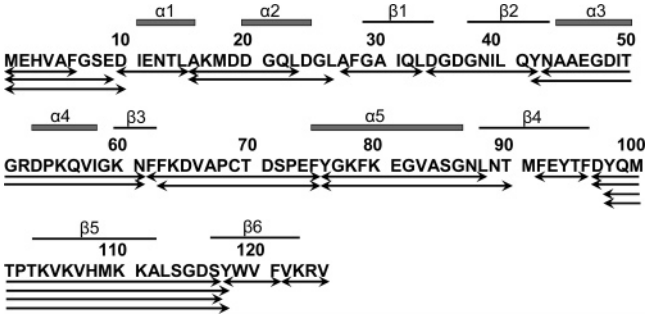

FIGURE 2: Peptic peptide fragments identified for PYP (wild-type and M100A). Peptic fragments are indicated by double-headed arrows under the sequence. Sequence regions corresponding to either α-helices or *β*-strands are shown above the gray bar and black line, respectively.

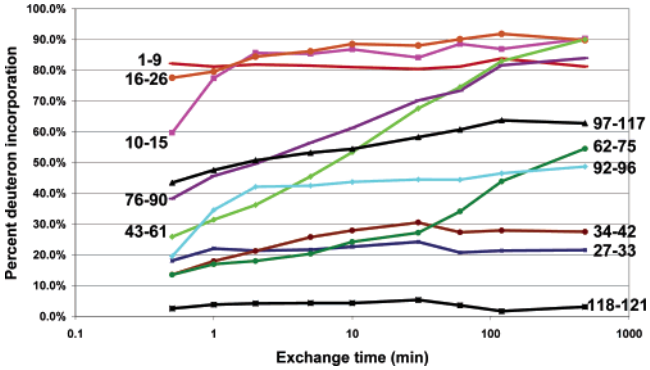

FIGURE 3: Time course for deuteron uptake by wild-type PYP peptic peptides. Exchange conditions: 5 mM sodium phosphate, pD 6.8.

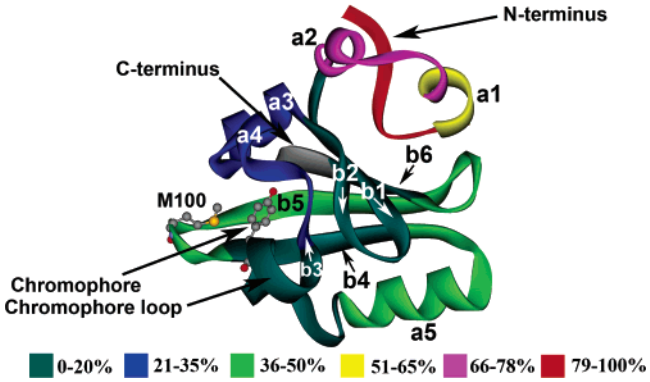

FIGURE 4: Color-coded three-dimensional structure of wild-type PYP. The color coding is in percent of peptide protons exchanged in 30 s. Peptide 122−125 is in gray and was not characterized by mass spectrometry. Exchange conditions are as in Figure 3. Secondary structure (a1−a5, α-helices 1−5; b1−b6, *β*-strands 1−6) was assigned by Swiss-Prot Deep View, using Protein Data Bank coordinates 2PHY.

to the dark state (*19*). In contrast, the M100A mutant is more than 90% in the I_2 states in blue light because of its relatively long-lived signaling state [lifetime of ∼5.5 min (*19*)]. Presumably, the difference in exchangeable hydrogens with wild type in the light and dark reflects those amide hydrogens whose accessibility, and thus exchange, is altered during the duration of the I_2 states. In the case of M100A, however, the duration of the I_2 states is ∼2000-fold longer than in the case of wild type, substantially increasing the probability of exchange.

Identification of Peptides. Unlabeled wild-type PYP was digested online by a pepsin column. Peptides were separated by HPLC and detected by mass spectrometry as described in Materials and Methods. Twenty-one peptides were identified, which cover 99% of the sequence (Figure 2). Peptides range from 4 to 21 amino acids, with an average peptide length of 10 residues. The peptides obtained from M100A are identical to those from wild type except for those containing M100. Also shown in Figure 2 are the locations of secondary structure in the amino acid sequence.

H/D Exchange of Wild-Type PYP. Among the 21 peptides identified following pepsin digestion, 11 nonoverlapping peptides were chosen for the analysis. The exchange kinetics (30 s to 480 min) of each of the 11 peptides characterized is summarized in Figure 3. To assist in describing the H/D exchange studies in structural terms, Figure 4 presents the structure of wild-type PYP (dark or resting state) with the various peptides in Figure 3 color coded using the extent of exchange at 30 s as the criteria. The detailed exchange data are presented in the supplementary tables in the Supporting Information and provide the quantitative basis for our analysis. Note that the sum of hydrogens exchanged by the peptides is less than for the intact protein because we have 11 peptides with N-termini which undergo back-exchange vs one N-terminus in the intact protein. In addition, five amino acids were not found in the peptides used (positions 91 and 122−125).

N-Terminal peptides 1−9, 10−15, and 16−26 are largely exchanged in less than 5 min, while the other peptides show more complex kinetics for the time range studied, with the exception of peptide 118−121, which is resistant to exchange. Peptide 1−9 is in a very flexible region of the protein, as shown by the X-ray crystallography (*4*) and the NMR solution structures (*6*) and would be expected to exchange rapidly. Peptide 10−15 encompasses the α-helix 1 region (Figures 2 and 4, a1). Nevertheless, the temperature factors from the X-ray structure (*4*) and rms deviation data from NMR (*6*) both suggest that this region is highly flexible if not unstable, consistent with our results. Note in Figure 3 that, at very early exchange times (30 s), peptide 10−15 (a1) has somewhat slower kinetics than peptide 1−9, indicative of some protection against exchange, but exchange is still largely complete within 5 min (Figure 3). Peptide 16−26 includes α-helix 2 (positions 20−24) (Figures 2 and 4, a2) as reported from the X-ray structure (*4*). However, this helix is one of the poorest defined regions in the NMR solution structure, with no evidence of a helix, and is highly accessible to solvent (*6*). Our results are consistent with the NMR data, as 78% exchange was reached by the first time point (30 s). Moreover, we find that the overlapping peptide 16−23 exchanged 95% of its amide hydrogens in 30 s (data not shown). It is clear from data for peptides 1−9, 10−15, and 16−26 that the N-terminal region of the wild-type PYP (positions 1−26) is solvent accessible and provides little resistance to exchange.

Immediately following the 27 N-terminal residues is the *β*-hairpin, which is made up of *β*-strands 1 (29−34) and 2 (37−43) (Figures 2 and 4, b1 and b2). The H/D exchange data for the two peptides overlapping this region (peptides 27−33 and 34−42) show slow exchange kinetics. After 8 h of exchange, the percentages of exchange of these two peptides remain at 22% (peptide 27−33) and 28% (peptide

34−42), an indication of stable hydrogen bonds in this region and low solvent accessibility. In terms of secondary structure, peptide 43−61 includes α-helix 3 (a3), α-helix 4 (a4), and the beginning of β-strand 3 (b3) (Figures 2 and 4). Importantly, this region includes E46, T50, and R52, all with side chains that interact with the PYP chromophore, directly or indirectly, through a hydrogen bond network (*4*). The H/D exchange data of this region reveal a pattern of gradual increase, in sharp contrast to peptide 1−9, whose exchange is essentially completed at or before our first time point (30 s), and peptide 118−121, whose exchange is extremely slow. This exchange pattern is indicative of intermediate protection against solvent exchange for most of the residues located within this region. This is consistent with the exchange data from NMR, in which both α-helix 3 (a3) and α-helix 4 (a4) are described as having intermediate exchange rates, and the exchange kinetics of β-strand 3 (b3) was determined to be fast (*6*).

Following peptide 43−61 is a loop containing C69 (peptide 62−75, Figure 4, chromophore loop), which is linked to the chromophore by a thioester bond. H/D exchange kinetics in this region is considerably slower than an unstructured region of secondary structure, such as in the case of peptide 1−9. This result suggests that in the dark state the backbone in this region is well organized, which is in agreement with the temperature factors in the X-ray crystallographic data (*4*). Peptide 76−90 is dominated by α-helix 5 (a5, also called the connecting helix, residues 76−85), the N-terminus of β-strand 4 (b4), and a small loop in between (Figures 2 and 4). The exchange kinetics in this region also have a combination of fast and intermediate exchange rates, consistent with NMR exchange data (*6*). The location of peptide 92−96, which is within β-strand 4 (Figures 2 and 4, b4), is on the external side of the central sheet, consistent with its intermediate protection against exchange with deuterated solvent.

Peptide 97−117 begins with the loop connecting β-strand 4 and β-strand 5 (residues 97−102), including the entire β-strand 5 (b5, 103−112), and ends with the connecting loop between β-strand 5 and β-strand 6 (113−116) (Figures 2 and 4). Almost one-half of the amide hydrogens in peptide 97−117 exchange during the 30 s incubation with deuterium. These exchanging hydrogens are presumably those in the loop regions (9 of the 19 amide hydrogens). When the exchange kinetics of peptide 97−117 are compared to the overlapping peptide 98−118, the former has 1.2 (1.6 after correcting for back-exchange) more exchangeable protons than the latter throughout the exchange time course. Peptide 97−117 contains one more amide proton from the loop between β-strand 4 (b4) and β-strand 5 (b5) and one less amide proton from β-strand 6 (b6). Because the difference in exchange is basically unchanged throughout the whole time course, it appears that a fast-exchanging amide proton (position 117) has been replaced by a slow-exchanging amide proton (position 118), consistent with β-strand 6 (b6) being extremely stable compared to loop regions. Peptide 118−121 exchange kinetics are extremely slow (Figure 3) and do not undergo any significant exchange in 8 h, consistent with β-strand 6 (b6) being very stable. The overlapping peptide 114−120 has a very slow exchange component (data not shown), which is presumably positions 117−120 in β-strand 6 (b6), and a fast exchanging component, which would be

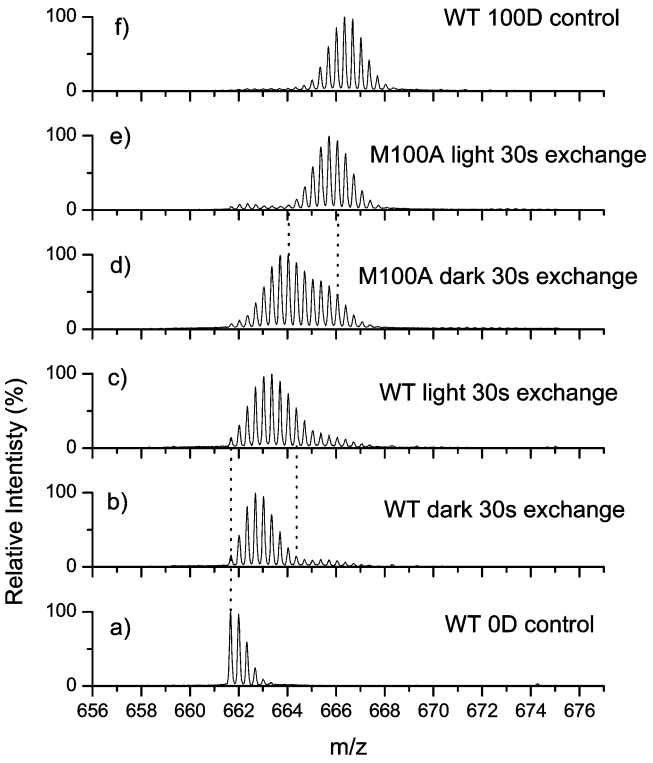

FIGURE 5: MS spectra of triply charged peptide 43−61. Exchange conditions are as in Figure 3. Panel a, wild-type PYP with no exchange; panel f, wild-type PYP under denaturing condition and long exchange time to allow complete exchange; panels b−e, as indicated on the figures.

positions 114−116 in the loop between β-strands (Figures 2 and 4).

Exchange Kinetics: Wild-Type Light minus Dark. From the mass shift of the peptide envelopes, deuterium uptake was calculated for both wild-type PYP and the M100A mutant in both the dark and blue light illumination. To illustrate the quality of the data, mass shift envelopes are shown in Figure 5 for peptide 43−61, for wild type and M100A in the light and dark. Light and dark deuterium uptakes by the 11 peptides characterized from the wild-type protein are summarized schematically in Figure 6 (panels a−c, wild-type dark; panels d−f, wild-type blue light) with the detailed data provided in the supplementary tables. It is apparent that the regions in which significant changes can be observed for dark vs light include α-helices 3 and 4 (peptide 43−61) in 30 s and 10 min (e.g., compare panels a and d and panels b and e), the chromophore loop (peptide 62−75) in 10 min and 8 h (e.g., compare panels b and e), and to a lesser extent at 8 h β-strands 1, 2, and 4 (compare panels c and f). The N-terminal region was observed to exchange extremely fast in both the light and the dark (Figures 3 and 4); thus any kinetic differences that occur in the first 30 s cannot be quantified.

Exchange Kinetics: Wild Type vs M100A in the Dark. The difference between the wild-type protein and the M100A mutant in the dark can be seen by comparing panels a−c to panels g−i in Figure 6. Indeed, M100A in the dark is more similar to wild type in blue light, than wild type in the dark, with increased exchange of α-helices 3 and 4 (peptide 43−61) at 30 s (compare panels a and g), α-helices 3 and 4 and the chromophore loop (peptide 62−75) at 10 min (compare panels b and h), β-strands 1 (peptide 27−33), 2 (peptide 34−

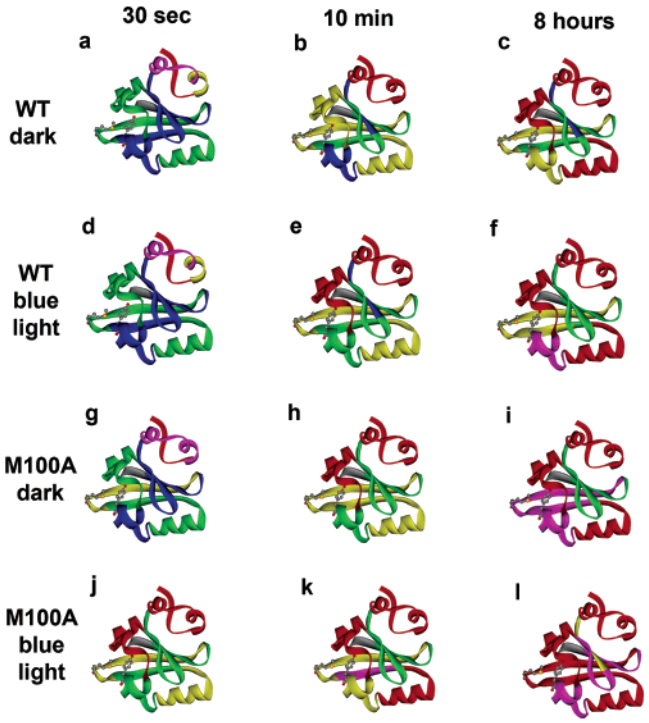

FIGURE 6: Color-coded three-dimensional structure of wild-type PYP and M100A as a function of time. Panels a−c, wild-type PYP exchanged in the dark; panels d−f, wild-type PYP exchanged with steady-state blue light illumination; panels g−i, M100A exchanged in the dark; panels j−l, M100A exchanged with steady-state blue light illumination. First column, exchanged for 30 s; second column, exchanged for 10 min; third column, exchanged for 8 h. Color coding in percent of peptide protons exchanged is as in Figure 4.

42), and 4 (peptide 92−96) and the chromophore loop (peptide 62−75) at 8 h (compare panels c and i). However, differences are observed, with peptides 10−15, 92−96 (β-strand 4), and 97−117 (β-strand 5) showing increased exchange at 30 s (compare panels a and g). The latter two peptides are in the immediate vicinity of the mutation, but clearly the impact of the mutation is propagated to the N-terminus (peptide 10−15).

Exchange Kinetics: M100A Light minus Dark. Following illumination of 20 μM M100A for 30 s with blue light, ~90% of the 446 nm absorbance is lost, with longer illumination having no further effect. Thus, the blue light steady state is ~90% I_2 states and ~10% dark state.

The changes in exchange kinetics between the dark and bleached states of M100A are shown by comparison of panels g−i with panels j−l in Figure 6. Bascially, all of the peptides, with the exception of peptides 1−9 and 118−121 (b6), have increased exchange in the illuminated M100A relative to the dark form at 30 s. Note that as a consequence of the broad ranges of exchange for each color used, peptides 27−33 (b1), 34−42 (b2), and 97−117 (b5) do not appear to change in Figure 6 (panels g and j) but in fact are significantly different numerically between the dark state and the signaling states (see supplementary tables in Supporting Information). Moreover, at 10 min and 8 h, a similar pattern is observed, with increased exchange on steady-state illumination of the mutant except for the N-terminal region (*1*−*26*) and peptide 118−121. Thus, illumination of M100A with blue light results in major changes in accessibility/stability of the secondary structural elements, consistent with a global destablization.

DISCUSSION

Steady-state blue light illumination of wild-type PYP significantly alters the H/D exchange kinetics with a net of 11 hydrogens exchanging more rapidly in 8 h (6 of the 11 in less than 30 s) (Figure 1). Using a similar approach, but measuring both backbone and side chain exchanges, Hoff and co-workers (*27*) found a difference of ~16 hydrogens. Moreover, the mutation of M to A at position 100 results in substantially enhanced exchange kinetics, with a net of 11 more hydrogens exchanging in 8 h (with all of the net increase occurring in 30 s) relative to wild type in the dark. What is most striking is the additional net 21 hydrogens that exchange in M100A with blue light illumination as compared to M100A in the dark. These results are consistent with a long-lived signaling state in M100A with a significant change in accessibility to exchange in a relatively large portion of the protein.

As can be seen in Figure 6 (panel a) the central sheet is most resistant to exchange in the first 30 s, while the N-terminus (positions 1−26) is most accessible. Over the 8 h period studied, this pattern is maintained with peptides 118−121 (b6), 27−33 (b1), and 34−42 (b2) quite resistant to exchange and peptides 92−96 (b4) and 97−117 (b5) somewhat resistant. In contrast, peptides 43−61 (a3, a4) and 76−90 (a5) almost completely exchange over the 8 h period. Note that peptide 62−75 (chromophore loop) is relatively resistant to exchange for the first hour, but not at later times (Figure 3). Furthermore, the two N-terminal helices (a1, a2) observed in the X-ray structure appear to be flexible, consistent with the NMR structure (*6*, *11*), suggesting that these elements of secondary structure are due to crystal packing forces in the X-ray structures.

On exposure of wild-type PYP to steady-state blue light, the most significant change relative to the dark at 30 s is an increase in the exchange of peptide 43−61 (a3, a4) (Figure 6, panel d). Residues Glu46, Thr50, and Arg52 are all located in peptide 43−61 (Figure 7) and are hydrogen bonded, directly or indirectly, to the chromophore. Y42, adjacent to this peptide, is also hydrogen bonded to the chromophore. The changes in this region are consistent with the isomerization of the chromophore disrupting the hydrogen-bonding network in this region. It should be noted that several different scenarios can cause this increase in exchange kinetics, including an increase in flexibility of the two helices due to the movement of the chromophore and the loss of interactions between the two helices and the chromophore. In all cases, the backbone hydrogen bonds of these two helices must be perturbed.

At 10 min and 8 h (Figure 6, panels e and f) the sequence of destabilization of the wild-type peptides in blue light is similar, but accelerated relative to the dark state. That is, peptides 43−61 (a3, a4), 62−75 (chromophore loop), 92−96 (b4), 27−33 (b1), and 34−42 (b2) exchange more rapidly and more extensively. Thus, the perturbation in the region of the chromophore, resulting from illumination, is propagated to other regions of the PYP, but with the β-strands still resistant to exchange. Since the N-terminal peptides (peptides 1−9, 10−15, and 16−26) are almost completely

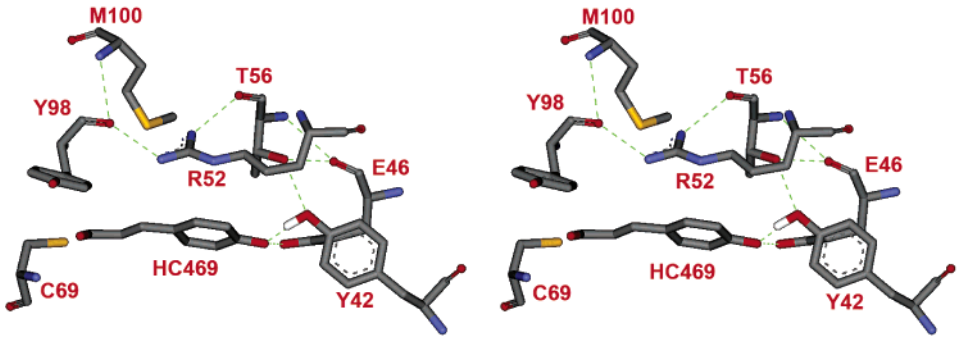

FIGURE 7: Hydrogen-bonding interaction in the chromophore binding pocket. Hydrogen bonds as assigned by Swiss-Prot Deep View, using Protein Data Bank coordinates 2PHY.

exchanged within 30 s in the dark, we cannot rule out that their rate of exchange increased on illumination. Indeed, the N-terminal region was observed to have a large perturbation upon blue light illumination in the NMR studies (*9*, *11*).

Compared with the wild type in the dark, the M100A mutant's exchange kinetics in the dark changes significantly, as can be seen in Figure 6 (panels g−i). However, the pattern of alteration is strikingly similar to the effect of illumination of the wild type, with the exception of the perturbation of peptides 92−96 (b4) and 97−117 (b5), which contain or are adjacent to the mutation at position 100, and peptide 10−15. Thus, the mutation in the M100A loop propagates a structural perturbation, presumably due to a structural change that modulates the interaction of the M100 loop (residues 98−102 in peptide 97−117) with key residues in peptide 43−61, across the central β-sheet and further destabilizes the N-terminus (peptide 10−15) relative to the wild type. It has been shown independently that the M100A mutant is destabilized compared with the wild type (*28*). The midpoint for denaturation by guanidine decreases from 2.73 M in the wild type, to 2.40 M in the mutant. Correspondingly, the melting temperature of the PYP decreases from 82 deg in the wild type to 68 deg in M100A (*29*).

Steady-state illumination of M100A with blue light leads to extensive changes in H/D exchange as shown in Figure 6 (panels j and k). The regions showing the largest extent of change are still the regions surrounding the chromophore, peptides 43−61 (a3 and a4) and 62−75 (chromophore loop). Moreover, the N-terminal region 1−26, where no differences were observed between the dark and illuminated states of wild type, reveals a destabilization. This is particularly apparent with peptides 10−15 and 16−26 (a1 and a2) at the early time points. At 30 s, 88% and 90% exchange were achieved at regions 10−15 (a1) and 16−26 (a2), respectively, compared with 75% and 78% in the dark. This change in kinetics indicates that the weak protection in the resting state is lost in the light. Regions 27−33 and 34−42, which encompass β-strands 1 and 2, respectively, and which displayed changes in exchange kinetics for the wild-type light and dark only at 8 h, now reveal exchange kinetic changes for M100A light vs dark after 10 min of exchange (Figure 6, panels h and k). Peptides 43−61 (a3, a4) and 62−75 (chromophore loop) have significant changes in exchange kinetics for wild-type dark and light, and this is amplified with M100A, particularly at 30 s, leading to full exchange of both peptides within 8 h. Regions 76−90 and 92−96 span the connecting helix (a5) and β-strand 4 (b4). Unlike wild type, changes in exchange kinetics on illumination were observed for 76−90 throughout the whole time course. The larger extent of difference of exchange kinetics in 76−90 suggests that the connecting helix (76−86) is affected to a much larger extent when there is a substantial population of I_2 states (see supplementary tables in Supporting Information).

Combining all of the data, the sequence of events on bleaching M100A with blue light appears to be photoisomerization, which is followed by perturbation of the chromophore binding pocket (α-helix 3, α-helix 4, and the connecting helix). This perturbation is quickly ($<$30 s) propagated to the disordered N-terminus (residues 1−26), which presumably swings away from the central sheet. This perturbation is subsequently propagated to other elements of the secondary structure. Thus, photoisomerization initiates a cascade of events that result in a global perturbation. Presumably with wild-type PYP (as opposed to M100A), there is sufficient stability retained in the core of the protein that the central sheet and the connecting helix remain intact in the relatively short-lived signaling state, and this is the structure that interacts with the response regulator to initiate signaling.

Models for the Formation of the Signaling State. Three different models have been proposed in the literature for structural changes upon photobleaching. In the "protein quake" model, a proton is transferred from E46 to the chromophore upon photobleaching, which increases the electrostatic energy of the buried E46 and initiates global conformation changes (*14*). Further experimental evidence, however, has shown that E46 is not directly linked to either protonation of the chromophore or the conformational changes leading to the signaling state (*2*) since mutant E46Q undergoes essentially the same photocycle with formation of the signaling state. In the "hydrophobic collapse" model (*7*), the space vacated by the movement of the chromophore aromatic ring on isomerization results in the movement of nearby hydrophobic side chains, which leads to distortion of the central β-sheet and the weakening of the interaction between the central sheet with the N-terminus. Consequently, the N-terminus moves away. In the "helix cap" model (*12*, *13*), the highly conserved N43 plays a central role in the transduction of structural change from the chromophore and surrounding regions to the N-terminus. Upon photoisomerization, the hydrogen bond between the side chain carbonyl of N43 and the backbone amide nitrogen of E46 is broken, which in turn weakens the hydrogen bonds between the side chain amide hydrogen of N43 to the backbone carbonyl oxygens of both F28 and L23, as well as the hydrogen bond

between the backbone amide of N43 and the D24 side chain. As a consequence, the interactions between the N-terminus and the rest of the protein are substantially weakened.

The H/D exchange data suggest a substantial disruption of the hydrogen bond network centered at the chromophore on illumination. Thus, interactions involving Y42, E46, T50, and R52 (Figure 7), and presumably the destabilization of the hydrogen bond from the R52 guanidinium group to the Y98 backbone carbonyl and N43 hydrogens bonds, are altered on illumination or mutation. It is notable from a comparison of M100A in the light and the dark that the hydrogen bonds within the central sheet are destabilized on illumination (Figure 6, compare panels j, k, and l to panels g, h, and i). Thus, increases in exchange kinetics in α-helix 3−4 and the central β-sheet, consequences predicted by both the helix cap and hydrophobic collapse models, are observed in our experiment. Therefore, our data here suggest that a combination of the two models is likely to be closer to the truth.

In summary, although the wild-type protein is only in the signaling state less than 10% of the time during steady-state illumination, regions of the protein that are affected by the dark to signaling state conversion are revealed by the H/D exchange kinetics. This is most striking in the regions hydrogen bonded to the chromophore and the loop containing the chromophore attachment site (peptides 43−61 and 62−75) and consistent with the NMR studies (*11*). Second, the M100A mutation, in addition to inhibiting dark recovery by almost 2000-fold, results in a structural change that perturbs peptide 43−61 at 30 s of exchange and peptide 62−75 at 10 min of exchange, consistent with a network of easily perturbed interactions between elements of secondary structure. Note that this perturbation qualitatively resembles the effect of steady-state illumination on the wild-type protein. Third, the H/D exchange comparison for the M100A mutant in the dark and with steady-state illumination reveals that the formation of the signaling state perturbs the structure of the protein in much the same way as the M100A mutation. However, illumination causes more extensive changes in exchange and accelerates the onset of the perturbations. Fourth, it is clear that both mutation and light drive a global destabilization of PYP. However, given that the signaling state has a relatively short half-life, it appears that the biologically relevant changes involve principally the chromophore binding and N-terminal regions.

ACKNOWLEDGMENT

We thank John Fitch for preparing PYP wild-type and M100A proteins and Dr. Terry E. Meyer for critical review of the manuscript and insightful discussion.

SUPPORTING INFORMATION AVAILABLE

Supplementary tables as described in the text. This material is available free of charge via the Internet at http://pubs.acs.org.

REFERENCES

1. Meyer, T. E., Yakali, E., Cusanovich, M. A., and Tollin, G. (1987) Properties of a water-soluble, yellow protein isolated from a halophilic phototrophic bacterium that has photochemical activity analogous to sensory rhodopsin, *Biochemistry 26*, 418−423.
2. Borucki, B., Devanathan, S., Otto, H., Cusanovich Michael, A., Tollin, G., and Heyn Maarten, P. (2002) Kinetics of proton uptake and dye binding by photoactive yellow protein in wild type and in the E46Q and E46A mutants, *Biochemistry 41*, 10026−10037.
3. Ujj, L., Devanathan, S., Meyer, T. E., Cusanovich, M. A., Tollin, G., and Atkinson, G. H. (1998) New photocycle intermediates in the photoactive yellow protein from *Ectothiorhodospira halophila*: picosecond transient absorption spectroscopy, *Biophys. J. 75*, 406−412.
4. Borgstahl, G. E., Williams, D. R., and Getzoff, E. D. (1995) 1.4 Å structure of photoactive yellow protein, a cytosolic photoreceptor: unusual fold, active site, and chromophore, *Biochemistry 34*, 6278−6287.
5. Genick, U. S., Soltis, S. M., Kuhn, P., Canestrelli, I. L., and Getzoff, E. D. (1998) Structure at 0.85 Å resolution of an early protein photocycle intermediate, *Nature (London) 392*, 206−209.
6. Duex, P., Rubinstenn, G., Vuister, G. W., Boelens, R., Mulder, F. A. A., Haard, K., Hoff, W. D., Kroon, A. R., Crielaard, W., Hellingwerf, K. J., and Kaptein, R. (1998) Solution structure and backbone dynamics of the photoactive yellow protein, *Biochemistry 37*, 12689−12699.
7. Cusanovich, M. A., and Meyer, T. E. (2003) Photoactive yellow protein: A prototypic PAS domain sensory protein and development of a common signaling mechanism, *Biochemistry 42*, 4759−4770.
8. Taylor, B. L., and Zhulin, I. B. (1999) PAS domains: internal sensors of oxygen, redox potential, and light, *Microbiol. Mol. Biol. Rev. 63*, 479−506.
9. Genick, U. K., Borgstahl, G. E. O., Ng, K., Ren, Z., Pradervand, C., Burke, P. M., Srajer, V., Teng, T.-Y., Schildkamp, W., McRee, D. E., Moffat, K., and Getzoff, E. D. (1997) Structure of a protein photocycle intermediate by millisecond time-resolved crystallography, *Science 275*, 1471−1475.
10. Rubinstenn, G., Vuister, G. W., Mulder, F. A. A., Dux, P. E., Boelens, R., Hellingwerf, K. J., and Kaptein, R. (1998) Structural and dynamic changes of photoactive yellow protein during its photocycle in solution, *Nat. Struct. Biol. 5*, 568−570.
11. Craven, C. J., Derix, N. M., Hendriks, J., Boelens, R., Hellingwerf, K. J., and Kaptein, R. (2000) Probing the nature of the blue-shifted intermediate of photoactive yellow protein in solution by NMR: Hydrogen-deuterium exchange data and pH studies, *Biochemistry 39*, 14392−14399.
12. Rajagopal, S., Anderson, S., Srajer, V., Schmidt, M., Pahl, R., and Moffat, K. (2005) A Structural pathway for signaling in the E46Q mutant of photoactive yellow protein, *Structure 13*, 55−63.
13. Ihee, H., Rajagopal, S., Srajer, V., Pahl, R., Anderson, S., Schmidt, M., Schotte, F., Anfinrud, P. A., Wulff, M., and Moffat, K. (2005) Visualizing reaction pathways in photoactive yellow protein from nanoseconds to seconds, *Proc. Natl. Acad. Sci. U.S.A. 102*, 7145−7150.
14. Xie, A., Kelemen, L., Hendriks, J., White, B. J., Hellingwerf, K. J., and Hoff, W. D. (2001) Formation of a new buried charge drives a large-amplitude protein quake in photoreceptor activation, *Biochemistry 40*, 1510−1517.
15. Borucki, B., Kyndt, J. A., Joshi, C. P., Otto, H., Meyer, T. E., Cusanovich, M. A., and Heyn, M. P. (2005) Effect of salt and pH on the activation of photoactive yellow protein and gateway mutants Y98Q and Y98F, *Biochemistry 44*, 13650−13663.
16. Borucki, B., Joshi, C. P., Otto, H., Cusanovich, M. A., and Heyn, M. P. (2006) The transient accumulation of the signaling state of photoactive yellow protein is controlled by the external pH, *Biophys. J.* (in press).
17. Joshi, C. P., Borucki, B., Otto, H., Meyer, T. E., Cusanovich, M. A., and Heyn, M. P. (2005) Photoreversal kinetics of the I_1 and I_2 intermediates in the photocycle of photoactive yellow protein by double flash experiments with variable time delay, *Biochemistry 44*, 656−665.
18. Ng, K., Getzoff, E. D., and Moffat, K. (1995) Optical studies of a bacterial photoreceptor protein, photoactive yellow protein, in single crystals, *Biochemistry 34*, 879−890.
19. Devanathan, S., Genick, U. K., Canestrelli, I. L., Meyer, T. E., Cusanovich, M. A., Getzoff, E. D., and Tollin, G. (1998) New insights into the photocycle of *Ectothiorhodospira halophila* photoactive yellow protein: photorecovery of the long-lived photobleached intermediate in the Met100Ala mutant, *Biochemistry 37*, 11563−11568.
20. Kyndt, J. A., Vanrobaeys, F., Fitch, J. C., Devreese, B. V., Meyer, T. E., Cusanovich, M. A., and Van Beeumen, J. J. (2003)

Heterologous pProduction of *Halorhodospira halophila* holophotoactive yellow protein through tandem expression of the postulated biosynthetic genes, *Biochemistry 42*, 965−970.
21. Genick, U. K., Devanathan, S., Meyer, T. E., Canestrelli, I. L., Williams, E., Cusanovich, M. A., Tollin, G., and Getzoff, E. D. (1997) Active site mutants implicate key residues for control of color and light cycle kinetics of photoactive yellow protein, *Biochemistry 36*, 8−14.
22. Wang, L., Pan, H., and Smith, D. L. (2002) Hydrogen exchange-mass spectrometry. Optimization of digestion conditions, *Mol. Cell. Proteomics 1*, 132−138.
23. Englander, J. J., Rogero, J. R., and Englander, S. W. (1985) Protein hydrogen exchange studied by the fragment separation method, *Anal. Biochem. 147*, 234−244.
24. Zhang, Z., and Marshall, A. G. (1998) A universal algorithm for fast and automated charge state deconvolution of electrospray mass-to-charge ratio spectra, *J. Am. Soc. Mass Spectrom. 9*, 225−233.
25. Smith, D. L., Deng, Y., and Zhang, Z. (1997) Probing the non-covalent structure of proteins by amide hydrogen exchange and mass spectrometry, *J. Mass Spectrom. 32*, 135−146.
26. Wales, T. E., and Engen, J. R. (2006) Hydrogen exchange mass spectrometry for the analysis of protein dynamics, *Mass Spectrom. Rev. 25*, 158−170.
27. Hoff, W. D., Xie, A., Van Stokkum, I. H. M., Tang, X.-j., Gural, J., Kroon, A. R., and Hellingwerf, K. J. (1999) Global conformational changes upon receptor stimulation in photoactive yellow protein, *Biochemistry 38*, 1009−1017.
28. Meyer, T. E., Devanathan, S., Woo, T., Getzoff, E. D., Tollin, G., and Cusanovich, M. A. (2003) Site-specific mutations provide new insights into the origin of pH effects and alternative spectral forms in the photoactive yellow protein from *Halorhodospira halophila*, *Biochemistry 42*, 3319−3325.
29. Meyer, T. E., Cusanovich, M. A., and Tollin, G. (1993) Transient proton uptake and release is associated with the photocycle of the photoactive yellow protein from the purple phototrophic bacterium *Ectothiorhodospira halophila*, *Arch. Biochem. Biophys. 306*, 515−517.

BI0608663